The influence of solvent additive on polymer solar cells employing fullerene and non-fullerene acceptors

Xin Song[1]*, Nicola Gasparini[1], Derya Baran[1]*

Physical Sciences and Engineering Division, KAUST Solar Center (KSC), King Abdullah University of Science and Technology (KAUST), KSC Thuwal 23955-6900, Saudi Arabia.

Corresponding author email: xin.song@kaust.edu.sa, derya.baran@kaust.edu.sa

Abstract:

Small molecule based non-fullerene acceptors (NFAs) are emerged as a new horizon to organic photovoltaics, due to their structural versatility, energy level tunability and ease of synthesis. High efficiency polymer donors have been tested with these non-fullerene acceptors in order to further boost the efficiency of organic solar cells. Most of the polymer:fullerene systems are optimized with solvent additives for high efficiency, while little attention has been spent on NFA based solar cells so far. In this report, we investigate the effect of the most common additive, 1,8-diiodooctane (DIO), on PTB7-Th:$PC_{71}BM$ solar cells and compare it with non-fullerene acceptor ITIC devices. It is interesting that the high boiling solvent additive does have a negative impact on the power conversion efficiency when PTB7-Th is blended with ITIC acceptor. We study the solar cell devices in terms of their optical, photo-physical and morphological properties and find out that PTB7-Th:ITIC devices with DIO results in coarser domains, reduced absorption strength and slightly lower mobility; while DIO improves the absorption strength of the PTB7-Th:$PC_{71}BM$ blend film and increase the aggregation of $PC_{71}BM$ in the blend, resulting in higher FF and J_{sc}.

With power conversion efficiency values (PCE) consistently surpassing the 10% threshold and improved photo-stability,[1] organic solar cells (OSCs) are becoming a promising candidate in thin-film photovoltaic technology.[2,3] One of the key component of an OSC is the photoactive layer which consists of donor and acceptor materials, mixing together to form the so-called bulk heterojunction (BHJ).[4,5] Fullerene derivate-based acceptors ([6,6]-phenyl C_{61}-/C_{71}-butyric acid methyl ester, $PC_{61}BM$ and $PC_{71}BM$ possess low absorption coefficient and narrow visible absorption window limiting the light-to-current generation, thus inhibiting the improvement of device performance.[6–12] In the past few years, non-fullerene electron acceptors (NFAs) have emerged as superior candidates as electron acceptors because of the possibility of tailoring their frontier molecular orbitals, molecular structure, and strong absorption profiles in the visible and NIR-range.[13-18] Now single-junction OSCs with a PCE> 13% has been recorded by Hou et al.[15] Among the high efficiency NFAs reported, 3,9-bis(2-methylene-(3-(1,1-dicyanomethylene)-indanone))-5,5,11,11-tetrakis(4-hexylphenyl)-dithieno[2,3-d:2’,3’-d’]-s-indaceno-[1,2-b:5,6b’]di-thiophene (ITIC) can obtain high efficiency values due to complementary absorption with the high/middle band gap donors.[17]

The effects of DIO have been well studied for polymer:fullerene solar cells.[22] In most cases, DIO not only enhances the aggregation of the polymer as it is a poor solvent for the polymer but also reduces the fullerene domain size as it is a good

solvent for fullerene derivatives.[23,24] Moreover, it can improve the mobility in the bulk as well as charge carrier collection for improved efficiency as it may facilitate the molecular packing.[25,26] Controlling the mixing of donor polymers with NFAs are difficult due to different mixing enthalpies, which has been investigated by Zhan et al,[27a] thus achieving an optimal microstructure that enable mixed and pure domains in NFA systems with solvent additives remains challenging.[27] We believe that common optimization methods adopted in fullerene based systems may not be valid for NFA solar cells.

In this work, we report the effect of the solvent additive 1,8-diiodooctane (DIO) in chlorobenzene (CB) solvent on the microstructure and photo-physical properties of poly[4,8-bis(5-(2-ethylhexyl)thiophen-2-yl)benzo[1,2-b;4,5-b']dithiophene-2,6-diyl-alt-(4-(2-ethylhexyl)-3-fluorothieno[3,4-b]thiophene-)-2-carboxylate-2-6-diyl)] (PBDTTT-EFT, or more commonly PTB7-Th) solar cell devices using $PC_{71}BM$ and ITIC as acceptors. By studying the optoelectronic characteristics of the devices together with microstructure analysis, we show that DIO has a beneficial effect on the performance of fullerene based solar cells. However, NFA devices depict lower performances when DIO is added, which is due to short circuit current (J_{sc}) and fill factor (*FF*) drop. We observe increased trap assisted recombination and slightly lower charge carrier mobility resulting from phase separated microstructure and increased roughness in PTB7-Th:ITIC films with CB/DIO mixed solvent.

For studying the additive effect in $PC_{71}BM$ and ITIC-based devices, we fabricate organic BHJ solar cells with a structure composing of indium tin oxide (ITO)/ZnO (~35 nm)/active layer/MoO_x (~5 nm)/Ag(~100 nm), where the thickness of PTB7-Th:$PC_{71}BM$ and PTB7-Th:ITIC active layers are ~100 nm and ~90 nm, respectively. **Figure 1** depicts the molecular structures of the materials used in this work. **Figure 2a** shows the current density versus voltage (*J*–*V*) characteristics of fullerene and NFA-based devices under AM1.5G illumination at 100 $mWcm^{-2}$. In agreement with previous reports,[28–30] PTB7-Th:$PC_{71}BM$ devices in chlorobenzene (CB) deliver poor PCE of 5.10% mainly due to low fill factor (FF) of 46.2%. Upon addition of 3% DIO, ~9% PCE is achieved as a result of improved J_{sc} (15.8 mA cm^{-2}) and *FF* (69.4%). On the contrary, PTB7-Th:ITIC solar cells processed from 3% DIO:97% CB depict an opposite behavior. (More details about the device optimization are shown in Figure S1 and Table S1) In fact, CB and 3% DIO-97% CB based devices deliver PCE of 7.62% and 5.43%, respectively. The drop in efficiency is mainly due to reduction of J_{sc} (13.7 $mAcm^{-2}$ to 11.6 $mAcm^{-2}$ in CB and 3% DIO, respectively) and FF (66.2% to 53.3% in CB and 3% DIO, respectively). **Table 1** summarizes the photovoltaic parameters of the solar cells studied in this work.

In order to investigate the different DIO effect in the fullerene and non-fullerene based systems, we first consider the J_{sc} evolution. Thus, we carried out external quantum efficiency (EQE) measurements. **Figure 2b** clearly shows the DIO effects

in these two systems. In particular, adding DIO into fullerene-based blend increases the light-to-current conversion in the all wavelengths region, resulting in an improved J_{sc} compared to the pristine devices. On the other hands, 3% DIO have a negative impact in the light harvesting of ITIC based solar cells, resulting in decreased EQE in the 300-800 nm range.

To better understand the negative effect of DIO on the photovoltaic parameters of PTB7-Th:ITIC devices in comparison to fullerene analogue, we investigate the optical and electrical properties of the BHJ films and devices as well as film morphology. The normalized absorption spectra of the blend films and neat materials (**Figure S2**) are recorded prior to metal deposition where the parasitic absorption of the non-active layers are considered as well. (**Figure 3a** and **b**) Only a small red-shift in the absorption maxima around 700 nm is observed which is similar to polymer solar cells processed with additives.[29] **Figure 3c** and **d** summarize the absorption strength of the film blends coated from chlorobenzene solution without and with 3% DIO. The absorption strength of PTB7-Th:$PC_{71}BM$ blend (3% DIO) increases between 400-700 nm region, which is consistent with the improved J_{sc} from device as well as recorded EQE spectra in **Figure 2b**, whereas PTB7-Th:ITIC film (3% DIO) has smaller absorption coefficient compared to the film without DIO (Figure 3d) within the same visible region, which is due to the different micromorphology and lower oscillation strength.[30-32] Notably, we also observe that

the small red-shift after the addition of DIO in ITIC based devices. We believe that the origin of this bathochromic shift is due to low solubility of PTB7-Th in DIO (< 0.2 mg/ml) compared to $PC_{71}BM$ (21 mg/ml) and ITIC (18 mg/ml), resulting in aggregation in thin film.[33]

To further characterize the significant decrease in FF, we turn our focus in understanding the effect of DIO on the recombination behavior of PTB7-Th:$PC_{71}BM$ and PTB7-Th:ITIC. First, we collect the *J-V* characteristics at different light levels (**Figure S2**) to study the J_{sc} and V_{oc} evolution of the solar cells as a function of light intensity.[34–36] In particular, J_{sc} generally follows a power-law dependence on light intensity (P^{in}) as $J_{sc} \propto P_{in}^{\alpha}$, where α represents a power-law exponent. In general, α=1 indicates that 2nd order recombination has a negligible effect on the charge extraction, whereas α<1 suggests that bimolecular recombination is the limiting factor. In **Figure 4a** it is apparent that bimolecular recombination is not the limiting factor in both fullerene and NFA-based systems since we calculate α values approaching the unity (Table S2). Following theoretical consideration, trap-assisted recombination is associated by a slope of 2 kT/q in a semi-logarithmic plot of V_{oc} vs P^{in}, while slope of kT/q represents signatures of purely bimolecular recombination. **Figure 4b** and **Table S2** clearly show that trap-assisted recombination decreases upon addition of DIO in fullerene based devices (1.77 kT/q vs 1.54 kT/q in CB and 3% DIO fullerene-based devices, respectively).

Conversely, we calculate higher slope value (1.57 kT/q and 1.79 kT/q in CB and 3% DIO ITIC-based devices, respectively), suggesting increased trap states formation upon DIO addition, which is detrimental for solar cells performance.[35]

In order to further investigate the photo-physics of PTB7-Th:$PC_{71}BM$ and PTB7-Th:ITIC, we study the charge transport ability by employing the technique of photo-induced by linearly increasing voltage (photo-CELIV).[37] With this technique we calculate the charge carrier mobility (μ) directly on the device without the fabrication of one-carrier type architecture (i.e. space charge limited current (SCLC) method[38]). In photo-CELIV the charge are photo-generated by a strongly absorbed laser pulse and extracted after an adjustable delay time. The transients are recorded by applying a 2V/60 μs linearly increasing reverse bias and a delay time of 10 μs. From the measured photocurrent transient we calculate the charge carrier mobility according to equation 1:

$$\mu = \frac{2d^2}{3At_{max}^2\left[1+0.36\frac{\Delta j}{j_0}\right]} \; if \; \Delta j \leq j_0 \qquad (1)$$

where d is the active layer thickness, A is the voltage rise speed =dU/dt U is the applied voltage, t_{max} is the time corresponding to the maximum of the extraction peak, and j_0 is the displacement current. From the transient in **Figure S3** it is clear that t_{max} occurs significantly earlier for 3% DIO-fullerene based and ITIC based solar cells in CB (2.6 μs and 2.7 μs, respectively) compared with PTB7-Th:$PC_{71}BM$ in CB and

3% DIO-ITIC devices (3.9 μs and 3.6 μs, respectively). As a result we calculate enhanced carrier mobility with and without DIO in fullerene based solar cells ($2.1x10^{-4}$ $cm^2V^{-1}s^{-1}$ and $9.6x10^{-5}$ $cm^2V^{-1}s^{-1}$, respectively), whereas, adding DIO in NFA systems has a negative impact in the charge mobility, ($1.9x10^{-4}$ $cm^2V^{-1}s^{-1}$ and $1.3x10^{-4}$ $cm^2V^{-1}s^{-1}$ in pristine and 3%DIO-ITIC based solar cells, respectively), in line with the FF values extracted from the *J-V* characteristics.

To correlate the optoelectronic properties of the devices with the structural information, we carry out bright-field transmission electron microscopy (BF-TEM). **Figure 5** shows BF-TEM images of PTB7-Th:$PC_{71}BM$ and PTB7-Th:ITIC blend films processed from chlorobenzene solutions without and with DIO additive. In agreement with previous reports,[29, 39] the TEM images of PTB7-Th:$PC_{71}BM$ blend (**Figure 5a**) clearly shows large domains (about 100–200nm in diameter) in the blend film prepared from CB, which is detrimental for charge transport. Differently, the morphology of blend film prepared from 3% DIO (**Figure 5b**) is more uniform. There is no large phase separation detected because of the high solubility of $PC_{71}BM$ in DIO solvent (~21 mg/ml), showing an interpenetrating network and reduce domain size. The TEM image of PTB7-Th:ITIC blend film processed without DIO additive, as shown in **Figure 5c**, reveals a bi-continuous and percolated morphology. As 3% DIO is added to the blend solution, the film forms interconnected, well-woven pathways for charge transport, (**Figure 5d**). We hypothesis that the different

property of ITIC as modest solubility in DIO solvent (~18 mg/ml), crystallinity and miscibility with PTB7-Th is the main reason for this phenomenon. The decreased photovoltaic properties, in particular FF, observed for this processing condition is resulted from less charge carrier photo-generation and hindered transport by this morphology where large-scale phase separation is seen. Moreover, the large domains may cause the significant vertical phase separation, which was supported by Wei et al.[40] However, these large domains may have a negative effect to the charge transport and collection because of the lower carrier mobility in the blend of PTB7-Th:ITIC (3% DIO) devices, thus obtaining poor performance.

Finally, we investigate the topography of the devices with and without additive by atomic force microscopy (AFM) technique. **Figure 6** shows the height and phase images of fullerene and NFA based systems. Clearly, PTB7-Th:$PC_{71}BM$ in CB (**Figure 6a-e**) depicts significant phase separation in line with the TEM images, differently, we observe a smooth surface after addition of 3% DIO (**Figure 6b-f**) beneficial for high performance devices.[39] Conversely, ITIC-based blends show a fine intermix when coated from CB and smoother surface (1.32 nm) (**Figure 6c-g**), while the addition of 3% DIO increased significantly the roughness of the blend (19.2 nm) (**Figure 6d-h**) and consequentially the probability of charge recombination, in line with the V_{oc} vs light intensity behavior.

In summary, we investigate the effect of DIO additive in the device performance and microstructure of the state-of-the-art PTB7-Th devices blending with fullerene and non-fullerene acceptor. Despite its positive effect in PTB7-Th:$PC_{71}BM$ blends due to reduction of the large fullerene domains, we observe a dramatically opposite situation for PTB7-Th:ITIC solar cell devices with the introduction of DIO. The reason of the drastic performance drop is the formation of a well-woven pathways for charge transport, which increases phase separation of the donor and acceptor matrix and surface roughness. We conclude that the common optimization conditions adopted in fullerene-based devices cannot be easily translated for NFA-based systems and new approaches are required for optimal nano-morphology.

Experimental section

Fabrication and Characterization of OSCs.

PTB7-Th and ITIC were purchased from 1-Materials Inc. $PC_{71}BM$ was purchased from Nano-C. For PTB7-Th:$PC_{71}BM$ solution, blend solution in a 25 mg/ml was prepared with a constant weight ratio of 1:1.5 in pure CB or mixed solvent with CB (97):DIO (3). For PTB7-Th:ITIC solution, blend solution in a 20 mg/ml was prepared with a constant weight ratio of 1:1.2 in pure CB or mixed solvent with CB

(97):DIO (3). These four solutions were stirring in the glove box with a temperature of 50 ^{o}C overnight.

Zinc oxide precursor solution was prepared by dissolving zinc acetate dihydrate ($Zn(CH_3COO)_2 \cdot 2H_2O$, 99%, Sigma) and ethanolamine ($NH_2CH_2CH_2OH$, 98%, Sigma) in 2-methoxyethanol ($CH_3OCH_2CH_2OH$, 98%, Sigma), then stirring the solution overnight. For device preparation, we firstly cleaned ITO substrates with detergent water, deionized water, acetone and isopropyl alcohol in an ultrasonic bath sequentially for 20 min. The ITO substrates were under UV-Ozone treatment for 30 min. After the UV-Ozone treatment, ZnO precursor solution was spin coated at 4000 rpm onto the ITO substrates. After being baked at 200 °C for 10 min in air, the ZnO-coated substrates were transferred into nitrogen-filled glove box. The PTB7-Th:$PC_{71}BM$ blend solution was spin coated with 2000 rpm) to obtain the thickness near 100 nm. The PTB7-Th:ITIC blend solution was spin coated with 1500 rpm to obtain the thickness near 90 nm. The device fabrication was completed by thermal evaporation of 5 nm MoO_x (Alfa) and 100 nm Ag (Kurt Lesker) at a pressure of less than $2x10^{-6}$ Pa. The active area of all devices was 0.1 cm^2 through a shadow mask. *J-V* measurements of solar cells were performed in the glovebox with a Keithley 2400 source meter and an Oriel Sol3A Class AAA solar simulator calibrated to 1 sun, AM1.5 G, with a KG-5 silicon reference cell certified by Newport. The external quantum efficiency (EQE) measurements were performed at zero bias by

illuminating the device with monochromatic light supplied from a Xenon arc lamp in combination with a dual-grating monochromator. The number of photons incident on the sample was calculated for each wavelength by using a silicon photodiode calibrated by NIST. All light intensity dependence measurements on *J-V* curves experiments were performed using the all-in-one measurement system PAIOS 3.2 (Fluxim).

Absorption spectra were acquired on a Carry 5000 UV-Vis-NIR spectrophotometer by Agilent Technologies. The thickness measurement is based on Tencor Profiler machine. A 5400 Agilent atomic force microscope (AFM) in tapping mode was used to measure the surface morphology of blend film. The transmission electron microscopy (TEM) images were performed using FEI instrument at 300 kV accelerating voltage. In photo-CELIV measurements, the devices were illuminated with a 405 nm laser-diode. Current transients were recorded across an internal 50 Ω resistor of an oscilloscope (Agilent Technologies DSO-X 2024A). We used a fast electrical switch to isolate the cell and prevent charge extraction or sweep out during the laser pulse and the delay time. After a variable delay time, a linear extraction ramp is applied via a function generator. The ramp, which was 60 μs long and 2 V in amplitude, was set to start with an offset matching the V_{oc} of the cell for each delay time.

References:

[1] N. Gasparini, M. Salvador, S. Strohm, T. Heumueller, I. Levchuk, A. Wadsworth, J. H. Bannock, J. C. de Mello, H.-J. Egelhaaf, D. Baran, I. McCulloch, C. J. Brabec, *Adv. Energy Mater.* **2017**, 1700770.

[2] H. Kang, G. Kim, J. Kim, S. Kwon, H. Kim, K. Lee, *Adv. Mater.* **2016**, *28*, 7821.

[3] L. Lu, T. Zheng, Q. Wu, A. M. Schneider, D. Zhao, L. Yu, *Chem. Rev.* **2015**, *115*, 12666.

[4] G. Li, R. Zhu, Y. Yang, *Nat. Photon.* **2012**, *6*, 153.

[5] S. Günes, D. Baran, G. Günbas, F. Özyurt, A. Fuchsbauer, N. S. Sariciftci, L. Toppare, *Sol. Energy Mater. Sol. Cells* **2008**, *92*, 1162.

[6] S. Holliday, R. S. Ashraf, A. Wadsworth, D. Baran, S. A. Yousaf, C. B. Nielsen, C.-H. Tan, S. D. Dimitrov, Z. Shang, N. Gasparini, M. Alamoudi, F. Laquai, C. J. Brabec, A. Salleo, J. R. Durrant, I. McCulloch, *Nat. Commun.* **2016**, *7*, 11585.

[7] S. Holliday, R. S. Ashraf, C. B. Nielsen, M. Kirkus, J. A. Röhr, C.-H. Tan, E. Collado-Fregoso, A.-C. Knall, J. R. Durrant, J. Nelson, I. McCulloch, *J. Am. Chem. Soc.* **2015**, *137*, 898.

[8] J. Jung, W. Lee, C. Lee, H. Ahn, B. J. Kim, *Adv. Energy Mater.* **2016**, 1600504.

[9] S. Li, L. Ye, W. Zhao, S. Zhang, S. Mukherjee, H. Ade, J. Hou, *Adv. Mater.* **2016**.

[10] C. B. Nielsen, S. Holliday, H.-Y. Chen, S. J. Cryer, I. McCulloch, *Acc. Chem. Res.* **2015**, *48*, 2803.

[11] D. Baran, S. Erten-Ela, A. Kratzer, T. Ameri, C. J. Brabec, A. Hirsch, *RSC Adv.* **2015**, *5*, 64724.

[12] D. Baran, S. Tuladhar, S. P. Economopoulos, M. Neophytou, A. Savva, G. Itskos, A. Othonos, D. D. C. Bradley, C. J. Brabec, J. Nelson, S. A. Choulis, *Synth. Met.* **2017**, *226*, 25.

[13] D. Baran, T. Kirchartz, S. Wheeler, S. Dimitrov, M. Abdelsamie, J. Gorman, R. S. Ashraf, S. Holliday, A. Wadsworth, N. Gasparini, P. Kaienburg, H. Yan, A. Amassian, C. J. Brabec, J. R. Durrant, I. McCulloch, *Energy Environ. Sci.* **2016**, *9*, 3783.

[14] D. Baran, R. S. Ashraf, D. A. Hanifi, M. Abdelsamie, N. Gasparini, J. A. Röhr, S. Holliday, A. Wadsworth, S. Lockett, M. Neophytou, C. J. M. Emmott, J. Nelson, C. J. Brabec, A. Amassian, A. Salleo, T. Kirchartz, J. R. Durrant, I. McCulloch, *Nat. Mater.* **2016**, *16*, 363.

[15] W. Zhao, S. Li, H. Yao, S. Zhang, Y. Zhang, B. Yang, J. Hou, *J. Am. Chem. Soc.* **2017**, *139*, 7148.

[16] A. Wadsworth, R. S. Ashraf, M. Abdelsamie, S. Pont, M. Little, M. Moser, Z. Hamid, M. Neophytou, W. Zhang, A. Amassian, J. R. Durrant, D. Baran, I. McCulloch, *ACS Energy Lett.* **2017**, *2*, 1494.

[17] Y. Lin, J. Wang, Z. Zhang, H. Bai, Y. Li, D. Zhu, X. Zhan, *Adv. Mater.* **2015**, *27*, 1170.

[18] Y. Lin, F. Zhao, Q. He, L. Huo, Y. Wu, T. C. Parker, W. Ma, Y. Sun, C. Wang, D. Zhu, A. J. Heeger, S. R. Marder, X. Zhan, *J. Am. Chem. Soc.* **2016**, *138*, 4955.

[19] T. Liu, L. Huo, X. Sun, B. Fan, Y. Cai, T. Kim, J. Y. Kim, H. Choi, Y. Sun, *Adv. Energy Mater.* **2016**, *6*, 1502109.

[20] H. Lu, J. Zhang, J. Chen, Q. Liu, X. Gong, S. Feng, X. Xu, W. Ma, Z. Bo, *Adv. Mater.* **2016**, *28*, 9559.

[21] H. Yao, Y. Cui, R. Yu, B. Gao, H. Zhang, J. Hou, *Angew. Chemie Int. Ed.* **2017**, *56*, 3045.

[22] Y. Liang, Z. Xu, J. Xia, S. T. Tsai, Y. Wu, G. Li, C. Ray, L. Yu, *Adv. Mater.* **2010**, *22*, 135.

[23] Y. Chen, X. Zhang, C. Zhan, J. Yao, *ACS Appl. Mater. Interfaces* **2015**, *7*, 6462.

[24] J. Zhao, S. Zhao, Z. Xu, B. Qiao, D. Huang, L. Zhao, Y. Li, Y. Zhu, P. Wang, *ACS Appl. Mater. Interfaces* **2016**, *8*, 18231.

[25] A. Foertig, J. Kniepert, M. Gluecker, T. Brenner, V. Dyakonov, D. Neher, C. Deibel, *Adv. Funct. Mater.* **2014**, *24*, 1306.

[26] S. Ben Dkhil, M. Pfannmöller, M. I. Saba, M. Gaceur, H. Heidari, C. Videlot-Ackermann, O. Margeat, A. Guerrero, J. Bisquert, G. Garcia-Belmonte, A. Mattoni, S. Bals, J. Ackermann, *Adv. Energy Mater.* **2017**, *7*, 1601486.

[27] a: P. Cheng, Y. Lin, N. K. Zawacka, T. R. Andersen, W. Liu, E. Bundgaard, M. Jørgensen, H. Chen, F. C. Krebs, X. Zhan, *J.Mater. Chem. A,* **2014**, 2, 19542. b: S. Dai, F. Zhao, Q. Zhang, T.-K. Lau, T. Li, K. Liu, Q. Ling, C. Wang, X. Lu, W. You, X. Zhan, *J. Am. Chem. Soc.* **2017**, 139, 1336. c: F. Zhao, S. Dai, Y. Wu, Q. Zhang, J. Wang, L. Jiang, Q. Ling, Z. Wei, W. Ma, W. You, X. Zhan, *Adv. Mater.* **2017**, 29, 1700144. d: Y. Lin, F. Zhao, Y. Wu, K. Chen, Y. Xia, G. Li, S. K. Prasad, J. Zhu, L. Huo, H. Bin, X, Zhan *Adv. Mater.* **2017**, 29, 1604155. e: Y. Lin, F. Zhao, Q. He, L. Huo, Y. Wu, T. C. Parker, W. Ma, Y. Sun, C. Wang, D. Zhu, A. J. Heeger, S. R. Marder, X. Zhan, *J. Am. Soc. Chem.*, **2016,** 138, 4655.

[28] N. Gasparini, L. Lucera, M. Salvador, M. Prosa, G. D. Spyropoulos, P. Kubis, H.-J. Egelhaaf, C. J. Brabec, T. Ameri, *Energy Environ. Sci.* **2017**, *10*, 885.

[29] Z. He, B. Xiao, F. Liu, H. Wu, Y. Yang, S. Xiao, C. Wang, T. P. Russell, Y. Cao, *Nat. Photon.*,**2015**, *9*, 174.

[30] N. Gasparini, X. Jiao, T. Heumueller, D. Baran, G. J. Matt, S. Fladischer, E. Spiecker, H. Ade, C. J. Brabec, T. Ameri, *Nat. Energy* **2016**, *1*, 16118.

[31] J. Peet, J. Y. Kim, N. E. Coates, W. L. Ma, D. Moses, a J. Heeger, G. C. Bazan, *Nat. Mater.* **2007**, *6*, 497.

[32] a: J. K. Lee, W. L. Ma, C. J. Brabec, J. Yuen, J. S. Moon, J. Y. Kim, K. Lee, G. C. Bazan, A. J. Heeger, *J. Am. Chem. Soc.* **2008**, *130*, 3619. b: R. Mondal, S. Ko, J. E. Norton, N. Miyaki, H. A. Becerril, E. Verploegen, M. F. Toney, J.-L. Brédas, M. D. McGehee, Z. Bao, *J.Mater. Chem.* **2009**, 19, 7195.

[33] C.-M. Liu, Y.-W. Su, J.-M. Jiang, H.-C. Chen, S.-W. Lin, C.-J. Su, U.-S. Jeng， K.-H. Wei, *J. Mater. Chem. A,* **2014**, 2, 20760.

[34] P. Schilinsky, C. Waldauf, C. J. Brabec, *Appl. Phys. Lett.* **2002**, *81*, 3885.

[35] M. M. Mandoc, F. B. Kooistra, J. C. Hummelen, B. De Boer, P. W. M. Blom, *Appl. Phys. Lett.* **2007**, *91*, 2005.

[36] N. Gasparini, M. Salvador, S. Fladischer, A. Katsouras, A. Avgeropoulos, E. Spiecker, C. L. Chochos, C. J. Brabec, T. Ameri, *Adv. Energy Mater.* **2015**, *5*, 1501527.

[37] A. Pivrikas, N. S. Sariciftci, G. Juška, R. Österbacka, *Prog. Photovoltaics Res. Appl.* **2007**, *15*, 677.

[38] V. Mihailetchi, J. Wildeman, P. Blom, *Phys. Rev. Lett.* **2005**, *94*, 126602.

[39] J. Zhang, Y. Zhang, J. Fang, K. Lu, Z. Wang, W. Ma, Z. Wei, *J. Am. Chem. Soc.* **2015**, *137*, 8176.

[40] D. Deng, Y. Zhang, J. Zhang, Z. Wang, L. Zhu, J. Fang, B. Xia, Z. Wang, K. Lu, W. Ma, Z. Wei *Nat. Commun.* **2016**, 7, 13740.

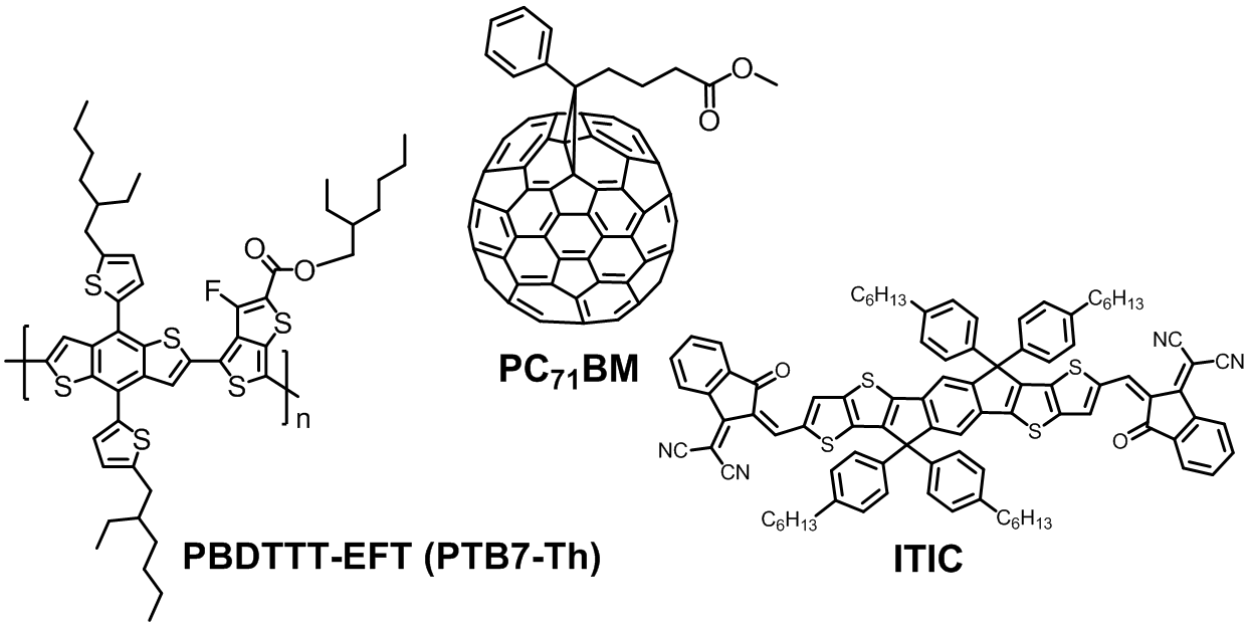

Figure 1. Chemical structures of the donor and acceptor molecules used in this study.

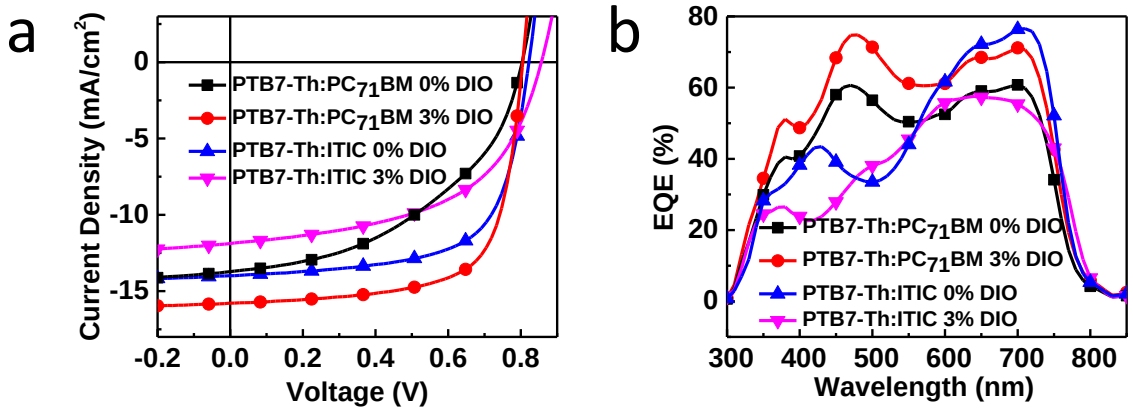

Figure 2. Current-voltage characteristics of PTB7-Th:$PC_{71}BM$ and PTB7-Th:ITIC devices without and with 3% DIO under 1 sun illumination and external quantum efficiency (EQE) spectra of the corresponding devices.

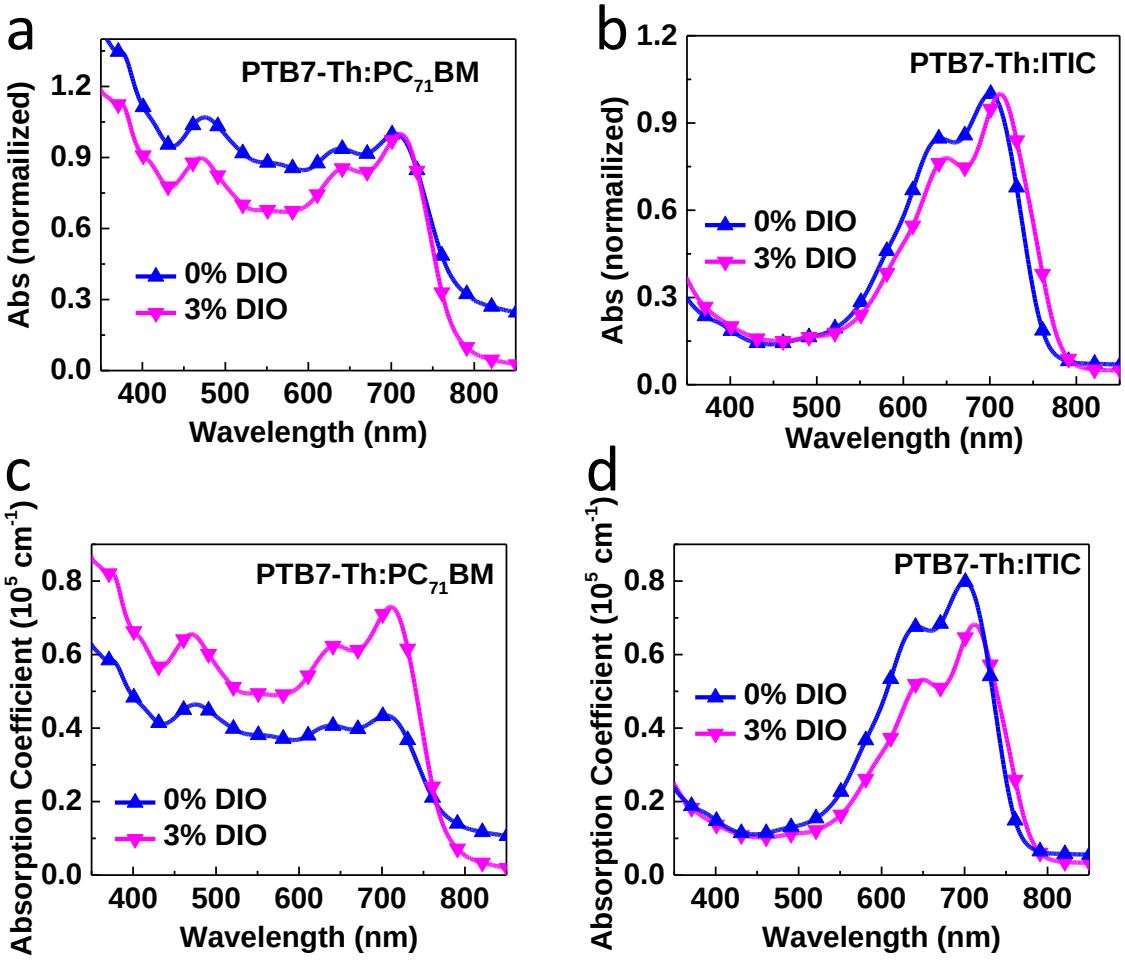

Figure 3. Optical properties of PTB7-Th:$PC_{71}BM$ and PTB7-Th:ITIC films without and with 3% DIO. a,b) Normalized absorption profiles of blend films. c,d)absorption strengths of blend films corrected for film thicknesses.

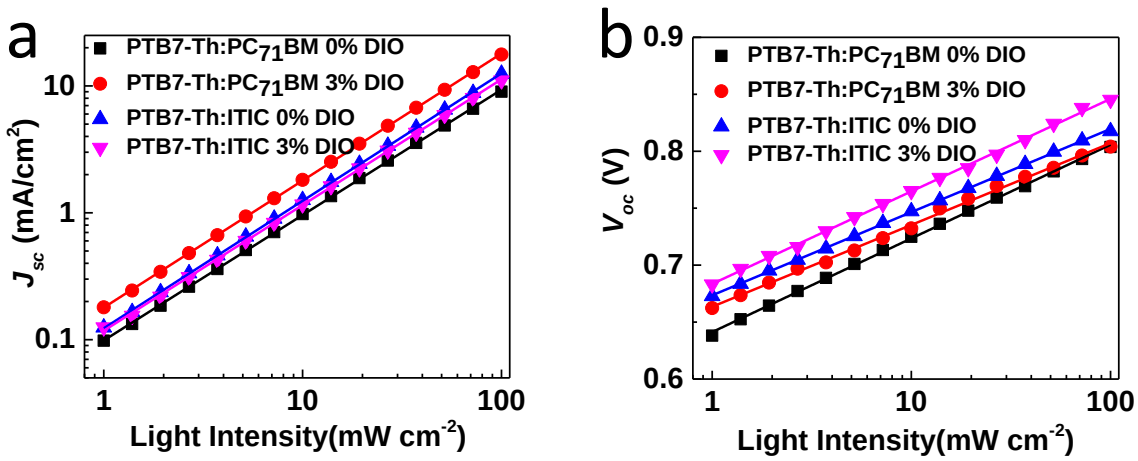

Figure 4. a) J_{sc} vs. light intensity and b) V_{oc} vs. light intensity measurements of PTB-Th:$PC_{71}BM$ and PTB7-Th:ITIC devices under various light illuminations.

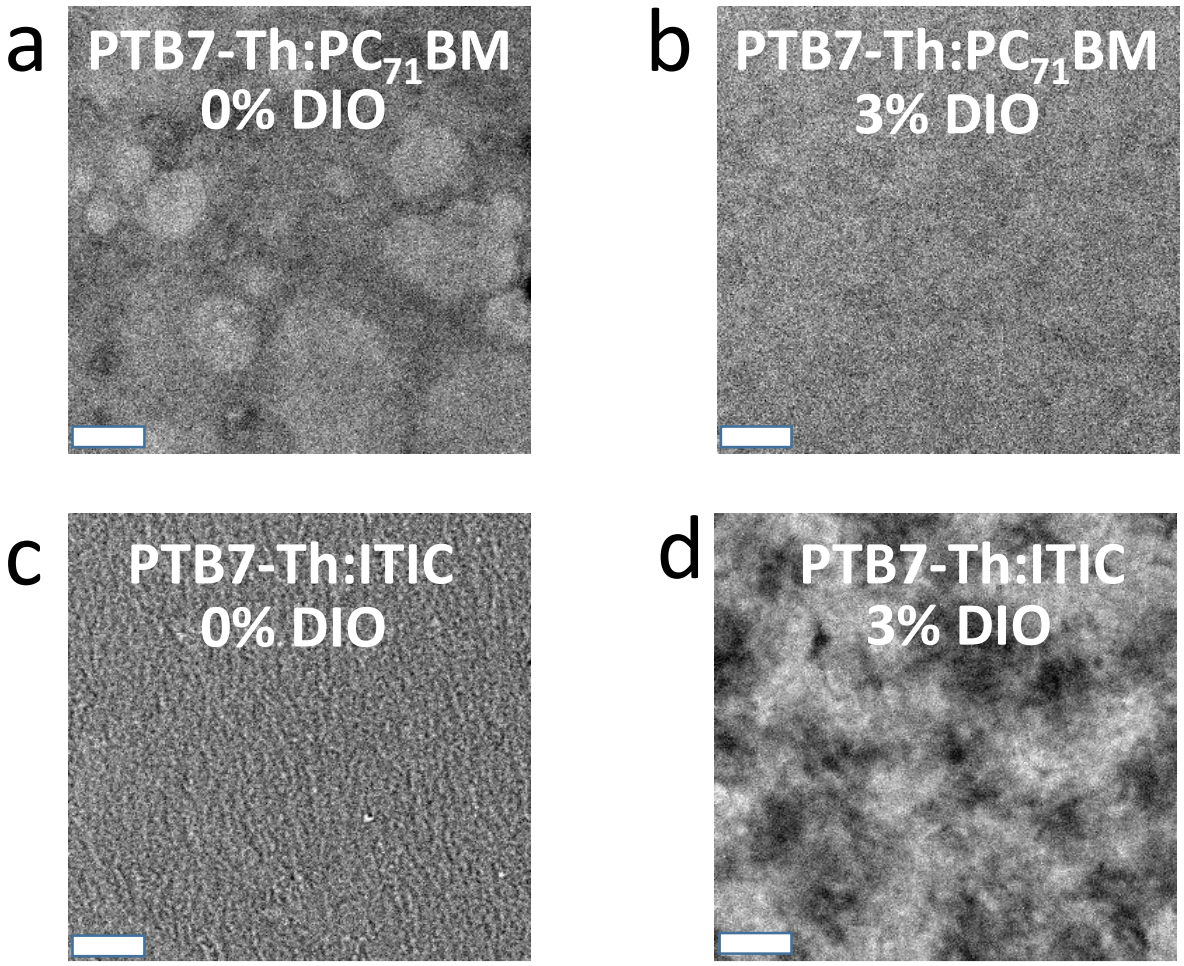

Figure 5. BF-TEM images of PTB7-Th:PC_{71}BM and PTB7-Th:ITIC blend films processed from chlorobenzene And 3% DIO as processing solvent additive. The scale bar represents 200nm.

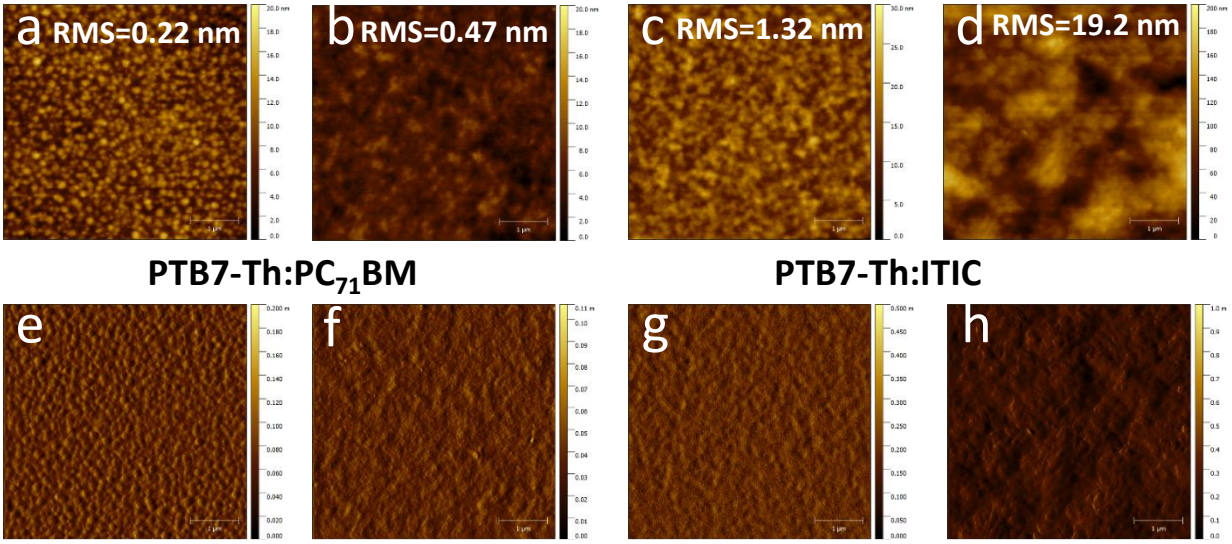

Figure 6. AFM topographical height and phase images of PTB7-Th:$PC_{71}BM$ (a-e and b-f of CB and 3% DIO, respectively) and PTB7-Th:ITIC films (c-g and d-h of CB and 3% DIO, respectively) processed from chlorobenene without and with 3% DIO additive, respectively . The size of image is 5 × 5 μm.

Table 1. Comparison of key photovoltaic parameters of PTB7-Th:$PC_{71}BM$ and PTB7-Th:ITIC devices without and with 3% DIO additive.

	J_{sc} (mA/cm^2)	**Integrated J_{sc} (mA/cm^2)**	**V_{oc} (mV)**	**FF (%)**	**PCE (%)**	**Ave PCE (%)**
PTB7-Th: $PC_{71}BM$ 0% DIO	13.7	13.2	804	46.2	5.10	4.9
PTB7-Th: $PC_{71}BM$ 3% DIO	16.1	15.8	805	69.4	8.96	8.8
PTB7-Th:ITIC 0% DIO	14.0	13.7	822	66.2	7.62	7.43
PTB7-Th:ITIC 3% DIO	11.9	11.6	857	53.3	5.43	5.21

TOC Figure

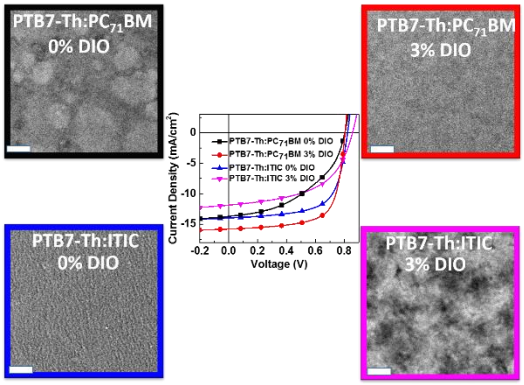
PTB7-Th:PC71BM
0% DIO
PTB7-Th:PC71BM
3% DIO
PTB7-Th:ITIC
0% DIO
PTB7-Th:ITIC
3% DIO
Current Density (mA/cm²)
Voltage (V)
PTB7-Th:PC71BM 0% DIO
PTB7-Th:PC71BM 3% DIO
PTB7-Th:ITIC 0% DIO
PTB7-Th:ITIC 3% DIO